

## LOAD BEARING CAPACITY OF BRACING MEMBERS WITH ALMOST CENTRIC JOINTS

Harald Unterweger\*

\* Institute of Steel Structures, Graz University of Technology, Austria  
e-mail: h.unterweger@tugraz.at

**Keywords:** Connections, Stability.

**Abstract.** *In building constructions for bracing members often hollow sections are used with slotted gusset plates at the ends. These plates are attached to non-stiffened plates of the adjacent construction. In practice sometimes a nearly centered joint is designed, by arranging the slotted gusset plate with an eccentricity of half the plate thickness to the member axis, so that the member eccentricity is minimised. In the paper the load bearing behaviour of such members under compression and tension is discussed based on numerical analysis with nonlinear FE – models including imperfections. The geometric parameters and boundary conditions are varied in such a way that practical cases are covered and that the typical load bearing behaviour can be seen. Based on these results an engineering model for the design in practice is represented.*

### 1 INTRODUCTION

Bracing members and truss members are often designed with hollow sections and slotted gusset plates at the ends. These plates are attached to non-stiffened plates of the adjacent construction, using welds or bolts. In Fig. 1a some typical joints of this type are represented, including also joints with concrete foundation. In Fig 1b the representative and idealized joint configuration for these joints - limited to rectangular hollow sections (RHS) - is shown. The vertical plate (KB2) is restrained in axis I. Here, the two different border cases related to boundary conditions are considered: - pinned (BC1) or, - fixed (BC2, e.g. "concrete joint" in Fig. 1a). The slotted gusset plate of the member is joined by a fillet weld (a1), passed around. An alternative solution with two bolt rows is possible, in accordance with the assumptions of the numerical analysis (fixed connection between plate KB1 and KB2 along their borders).

A special feature of the studied joint is the eccentric position of the slotted gusset plate with an eccentricity of half the plate thickness  $t_{KB1}$ , as shown in Fig. 1b. In doing so, the eccentricity of the RHS - member for the buckling check - relevant is member buckling out of plane (about the z - axis) - is minimised ( $e^* = 0,5 \cdot t_{KB2}$ ). The bending moment along the member-length is constant.

Based on the minimised eccentricity for the RHS - member, the opinion of practitioners is that only a buckling check for the member under axial load is necessary to get the load carrying capacity of the member. The results of this study will show that this approach would lead to high overestimations of the load carrying capacity, especially for low slenderness ratios of the member. The reason for this, are high bending moments in the gusset plate out of plane.

The loading of the RHS - member in this study is restricted to axial forces with bending moments only due to eccentricities of the joints. This paper summarizes the results in [1].

### 2 LOAD BEARING BEHAVIOUR OF THE MEMBER IN COMPRESSION

In the following the load bearing behaviour of the member in compression, influenced by the specific type of joint, is represented.

First of all the finite element (FE) – model and the executed nonlinear numerical analysis is presented. Afterwards the studied band width of the varied geometric parameters is summed up. At the end the results of the numerical nonlinear calculations for an example of a rectangular hollow section are presented, for different member slenderness and boundary condition.

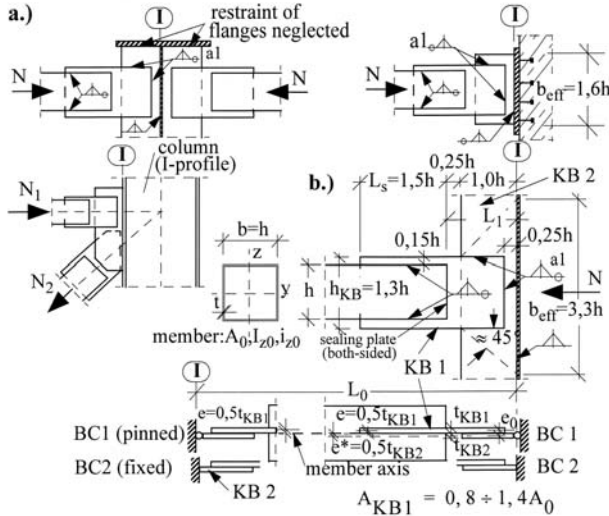


Figure 1: Studied RHS - member joints: a.) different types in practice, b.) geometry and restraint conditions of the studied representative joint.

## 2.1 FE model and calculation procedure

The numerical FE – model, based on the Software ABAQUS [2], consists of continuum (solid) and beam elements and is represented in Fig. 2a. The linear continuum elements were used within the joint and for the following parts of the hollow section (over a length of about 0,5 m). For the vertical gusset plates eight elements over the thickness were considered, because the localized plastification in this region affects highly the load bearing behaviour of the member. The continuation of the RHS - member was modeled with linear beam elements only to the section at midspan, because symmetric or antisymmetric boundary conditions there were sufficient to capture the real member behaviour. The boundary conditions at the end of the gusset plate (axis I) were chosen adjusted on the two studied configurations, pinned or fixed out of plane (see Fig. 1b). The two gusset plates were joined using contact elements along the axis of the weld in between. The sealing plates were omitted.

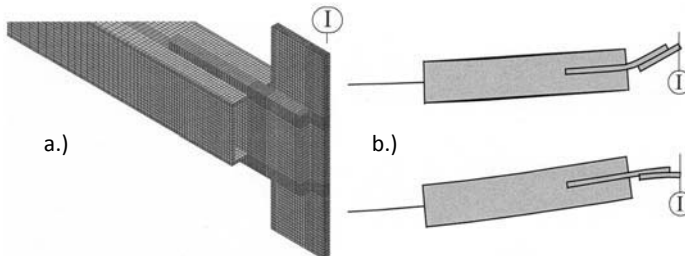


Figure 2: a.) FE – model of the joint, b.) relevant first eigenmode,  $L_0 = 2$  m, for a pinned (above) and fixed gusset plate (below).

In the study a squared, hot finished, RHS - profile with 100 / 100 / 5 mm was used, leading to gusset plate dimensions of 250 / 130 mm (KB 1) and 100 / 330 mm (KB 2). The calculations were done for total member lengths  $L_0 = 2, 3, 4, 5, 6, 7$  and 8 m. The corner radii of the hollow section were omitted, leading to an area  $A_0 = 1900 \text{ mm}^2$  and a radius of gyration  $i_{z,0} = 38,84 \text{ mm}$ .

In the calculations an ideal elastic – perfectly plastic material behaviour was considered with a characteristic yield strength of  $f_y = 235 \text{ N / mm}^2$ . A modulus of elasticity  $E = 210000 \text{ N/mm}^2$  and a Poisson ratio of  $\nu = 0,3$  were used.

First of all an LBA – analysis (**linear buckling analysis**) was made, leading to the capacity  $N_{LBA}$  of the member. Based on these results, on the one hand the “real” buckling lengths of the members were determined (using the formula for the Euler buckling load for the RHS - member section). Due to the limited bending stiffness of the gusset plates, the buckling length  $L_{cr,0}$  of the idealized RHS - member within the end – restraint in axis I ( $L_{cr,0} = L_0$  for BC 1,  $L_{cr,0} = 0,5 L_0$  for BC 2) is too small.

Afterwards the results are either based on the idealised slenderness  $\bar{\lambda}_{z,0}$  (Equ.1), with  $L_{cr} = L_0$ , or on the slenderness based on the LBA – analyses  $\bar{\lambda}_{LBA}$  (Equ. 2).

$$\bar{\lambda}_{z,0} = \sqrt{\frac{f_y}{\sigma_{cr,0}}} = \frac{L_0}{i_{z,0}} \cdot \frac{1}{\pi \cdot \sqrt{E/f_y}} = \frac{L_0}{i_{z,0}} \cdot \frac{1}{93,9} \quad (1)$$

$$\bar{\lambda}_{LBA} = \sqrt{\frac{N_{pl,0}}{N_{LBA}}} = \sqrt{\frac{A_0 \cdot f_y}{N_{LBA}}} \quad (2)$$

On the other hand the eigenmodes of the LBA – analyses, scaled to a maximum value of  $w_{\max} = L_0 / 1000$  were used for a GMNIA – analyses (**geometric and material nonlinear analyses with imperfections**). This was done with care, considering different eigenmodes (not only the one for the minimum ideal buckling load), to get a minimum for the load carrying capacity  $N_R$  of the member. In Fig. 2b the relevant eigenmodes for a member with small length  $L_0$  is shown for the two different boundary conditions. Additional GMNA – calculations were used to check the GMNIA – results. Residual stresses were ignored, because they affect the buckling capacity of RHS – members not significantly (e.g. [4]).

Also for cold formed RHS - members the presented results mainly are valid, only for high slenderness ratios – where the overall buckling of the member is relevant – the appropriate buckling curve should be used (e.g. curve *c* instead of *a*, using Eurocode 3 [3]).

## 2.2 Studied joint parameters

The numerical study was limited to rolled RHS – members. The joint geometry is restricted to the dimensions of Fig. 1b. Very important is the slotted length  $L_s \geq 1,5 \cdot h$  in the RHS – member. Otherwise sometimes significant smaller load bearing capacities would occur. The overlapping length of the two gusset plates was fixed with  $0,75 \cdot h$ . The distance between member end and restraint axis I is limited to  $L_1 = 1,25 \cdot h$ .

The thickness of the two gusset plates was varied in such a way that the area ratio  $A_{KB1} / A_0 = 0,8$  to  $1,4$  and  $t_{KB2} = (0,5 \text{ to } 1,0) \cdot t_{KB1}$ .

## 2.3 Results of the nonlinear calculations

The results of the nonlinear calculations for different member length (i.e. different member slenderness) and gusset plate thicknesses are presented in Fig. 3, based on an effective width of  $b_{\text{eff}} = 3,3 \cdot h = 330 \text{ mm}$  of gusset plate KB2. The load carrying capacity  $N_R$  is related to the section capacity of the RHS - member  $N_{pl,0} = A_0 \cdot f_y = 19,0 \cdot 23,5 = 446,5 \text{ kN}$ . The slenderness ratio  $\bar{\lambda}_{LBA}$  (Equ. 2) is based on the results of the LBA – analysis - that means based on the “real” buckling length.

In Fig. 3a the overall carrying behaviour is shown, based on the GMNA – results, without geometric imperfections. The effect of these geometric imperfections is quantified in Fig. 3b, where the results with and without imperfections are visible. It can be seen that the reduction of load carrying capacity is comparatively small.

In Fig. 3 also the buckling curve *a*, relevant for the buckling load capacity of a hot finished, RHS – member under only axial load in Eurocode 3 [3] is plotted (dotted line). It can be seen that the special feature of the studied joint – minimising of the member eccentricity – is only usable for high slenderness ratios and thick gusset plates. For example with a gusset plate thickness of  $t_{KB1} = t_{KB2} = 12$  mm, leading to a ratio  $A_{KB1} / A_0 = 0,82$  a dramatic reduction of the load carrying capacity occurs in case of the pinned gusset plate KB2, also for very low slenderness ratios ( $N_R \approx 0,16 \cdot N_{pl,0}$ ). A fixed gusset plate, however, increases the load carrying capacity significantly, but also for very low slenderness ratios the capacity is far below the section capacity of the RHS - member ( $N_R \approx 0,54 \cdot N_{pl,0}$ ). Not before the plate thickness is increased significantly ( $t_{KB1} = t_{KB2} = 20$  mm, leading to a ratio  $A_{KB1} / A_0 = 1,37$ ) and the gusset plate is fixed (BC2 in Fig. 1b) nearly about 80 % of the section capacity  $N_{pl,0}$  for small slenderness ratio is available.

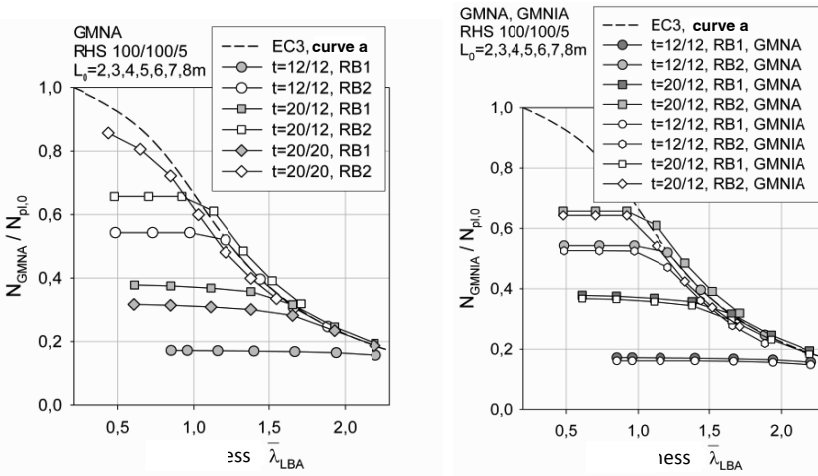


Figure 3: a.) GMNA - results depending on the slenderness ratio, b.) GMNA - results in comparison with GMNIA - results, for pinned (RB1=BC1) and fixed (RB2=BC2) gusset plates.

The significant reduction of the load carrying capacity – also related to the buckling capacity of the RHS–member (see Fig. 3) – is caused by the local bending moments in the gusset plate, particularly at the end of the RHS – member. This can be seen in Fig. 4 for a very short member with the thin gusset plates mentioned before. In Fig 4a the pinned and in Fig. 4b the fixed ended gusset plate can be seen at the ultimate limit state. The gusset plate section at the member end reaches its section capacity under axial force and bending moment.

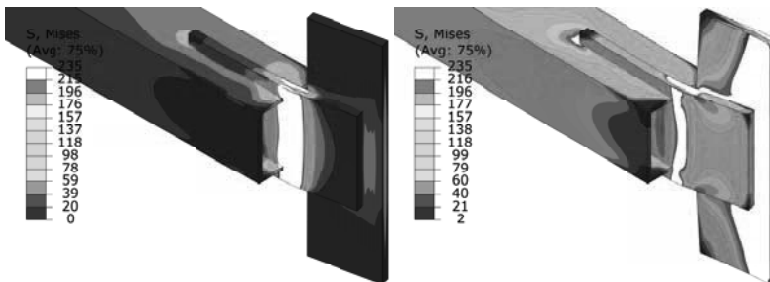


Figure 4: Short member ( $L_0 = 2$  m) at ultimate limit state (GMNA-analysis) with  $t_{KB1} = t_{KB2} = 12$  mm; a.) pinned gusset plate –  $N_{GMNA} / N_{pl,0} = 0,173$ , b.) fixed gusset plate –  $N_{GMNA} / N_{pl,0} = 0,543$ .

Summing up, the load carrying capacity of the RHS - member with the specific joint configuration of Fig. 1b has an upper limit – also for very low slenderness ratios – which primarily is influenced by the gusset plate thickness  $t_{KB1}$  and the boundary condition of the gusset plate (pinned or fixed). The influence of the effective width  $b_{eff}$  of the gusset plate is significant smaller.

These correlations are presented in Table 1. The tabulated load carrying capacities are calculated with the engineering model presented in chapter 4.

Table 1: Ratios of maximum compression capacities  $N_{1,Rd} / N_{pl,0}$  of the member – influence of gusset plate thickness  $t_{KB1}$  and boundary condition ( $t_{KB2} = 12$  mm).

boundary condition	$t_{KB1} = 12$	$t_{KB1} = 20$	$t_{KB1} = 25$	$t_{KB1} = 30$
	$A_{KB1}/A_0=0,82$	$A_{KB1}/A_0=1,37$	$A_{KB1}/A_0=1,71$	$A_{KB1}/A_0=2,05$
BC 1, $b_{eff} = 3,3h$	0,172	0,373	0,506	0,642
BC 2, $b_{eff} = 1,6h$	0,351	0,469	0,576	0,695
BC 2, $b_{eff} = 3,3h$	0,458	0,545	0,631	0,736

### 3 LOAD BEARING BEHAVIOUR OF THE MEMBER IN TENSION

The load bearing behaviour of the member in tension was also studied. Now the tension axial force reduces the bending moment in the relevant gusset plate section at the member end significantly (2<sup>nd</sup> order effect). The influence of the boundary condition (BC1 or BC2) disappears nearly complete and for the studied gusset plate thicknesses the following member capacities in tension were calculated ( $L_0 = 2$  m,  $b_{eff} = 330$  mm):

- $t_{KB1} = t_{KB2} = 12$  mm:  $N_{GMNA} / N_{pl,0} = 0,87$
- $t_{KB1} = t_{KB2} = 20$  mm:  $N_{GMNA} / N_{pl,0} = 0,94$
- $t_{KB1} = 20$ ,  $t_{KB2} = 12$  mm:  $N_{GMNA} / N_{pl,0} = 0,94$

### 4 ENGINEERING MODEL FOR COMPRESSION CAPACITY OF THE MEMBER

Based on the results of the numerical study, an engineering model was developed to calculate the compression load-bearing capacity of the RHS - member with the specific joint configuration of Fig 1b. It includes the following variations of the relevant parameter: - pinned (BC1) or fixed (BC2) end of the gusset plate, -  $b_{eff} = 1,6h$  to  $3,3h$ , - a “free” length of gusset plate  $L_1$  also longer than  $1,25h$ , - varying thicknesses, but  $t_{KB1} \geq t_{KB2}$ .

The engineering model includes on the one hand a conventional member buckling check with the specifications given in chapter 4.1 – relevant for high slenderness ratios – leading to  $N_{2,Rd}$ .

On the other hand the calculated capacity  $N_{2,Rd}$  is limited by an upper limit  $N_{1,Rd}$  – independent of the member slenderness – characterising the plateau of the load bearing capacity for small and medium slenderness (see Fig. 3). The resulting compression load bearing capacity  $N_{Rd}$  is the minimum of both values.

As stated in Eurocode 3 [3], a partial safety factor  $\gamma_f = 1,0$  is considered, leading to the design yield strength  $f_{yd} = f_y$  and the load capacity  $N_{Rd}$ .

#### 4.1 Buckling member capacity $N_{2,Rd}$

Although the “real” buckling length  $L_{LBA}$  of the member is influenced by the smaller bending stiffness of the gusset plates, the following simplifications are possible. For the buckling check about the  $z$  – axis only the member section is relevant ( $A_0$ ,  $i_{z0}$ ) and the relevant buckling curves of the international codes can be used (e.g. for hot finished, RHS – profiles, curve  $a$  in Eurocode 3 [3]).

For pinned gusset plates (BC1) simplified  $L_{LBA} = L_0$ , as long as  $L_1 < 1,5 \cdot h$ . In addition the constant moment  $M = N_{2,Rd} \cdot e^* = N_{2,Rd} \cdot (t_{KB2} / 2)$  (see Fig. 1b) should be used in the buckling check. For higher slenderness ratios the influence of the moment decreases and it can be omitted.

For fixed (BC2) gusset plates the eccentricity  $e^*$  can be omitted, if  $L_{LBA} = L_0$  is used. This simplification leads to conservative results, mainly for high thicknesses  $t_{KB1}$  (see Table 2). Otherwise the moment should be included ( $L_{LBA} \approx 0,85 \cdot L_0$ , as long as  $N_{2,Rd}$  is relevant for design).

#### 4.2 Upper limit for the member capacity – $N_{1,Rd}$

The engineering model for the upper limit capacity  $N_{1,Rd}$  of the member is defined by the load carrying capacity of the gusset plate – section at the end of the member (axis II), considering 2<sup>nd</sup> order effects. The model is summed up in Fig. 5.

The load bearing capacity  $N_{1,Rd}$  is based on the full utilization of the plastic section capacity, due to axial force and bending moment. As defined in Eurocode 3 [3], the acting axial force is considered by a reduced moment capacity  $M_{N,Rd}$ , given in Equ. 3 ( $f_{yd}$  is the design yield strength).

$$M_{N,Rd} = M_{pl,KB1} \cdot \left( 1 - \left( \frac{N_{1,Rd}}{N_{pl,KB1}} \right)^2 \right) = \frac{h_{KB} \cdot t_{KB1}^2}{4} \cdot f_{yd} \cdot \left( 1 - \frac{N_{1,Rd}^2}{h_{KB}^2 \cdot t_{KB1}^2 \cdot f_{yd}^2} \right) \quad (3)$$

To calculate  $N_{1,Rd}$  an iterative approach is necessary, until Equ. 4 is fulfilled.

$$M_{II} \leq M_{N,Rd} \quad (4)$$

The acting bending moment  $M_{II}$  in the gusset plate, depends on the axial force  $N_{1,Rd}$  and the actual boundary condition. For pinned gusset plates (BC1) the full eccentricity  $e_0$  is relevant in section II (see Fig. 5), leading to Equ. 5. The 2<sup>nd</sup> order effect, is covered by the factor  $f_{II}$  in form of a so called “Dischingerfaktor”, including the Euler buckling load  $N_{cr,BC1}$  for the gusset plate (Equ. 6), based on the relevant buckling length  $l_{cr} = 2 \cdot L_1$ .

$$M_{II} = N_{1,Rd} \cdot e_0 \cdot f_{II} = N_{1,Rd} \cdot \left( \frac{t_{KB1} + t_{KB2}}{2} \right) \cdot \frac{1}{1 - \frac{N_{1,Rd}}{N_{cr,BC1}}} \quad (5)$$

$$N_{cr,BC1} = \frac{\pi^2 \cdot E \cdot I_{z,KB1}}{l_{cr}^2} = \frac{\pi^2 \cdot E \cdot h_{KB} \cdot t_{KB1}^3}{48 \cdot L_1^2} \quad (6)$$

For fixed gusset plates (BC2) the bending moment due to the full eccentricity  $e_0$  is reduced, because also section I gets a part of this moment, leading to Equ. 7.

$$M_I + M_{II} = N_{1,Rd} \cdot e_0 \quad (7)$$

For the two parts in Equ. 7 the bending stiffness of the two gusset plates is relevant (identical bending deformations). This gives:  $M_I / M_{II} = I_{z,KB2} / I_{z,KB1}$ , where  $I_i$  are the moment of inertias. Based on Equ. (7), finally we get  $M_{II}$  using Equ. (8b). But now the Euler buckling load  $N_{cr,BC2}$  (Equ. 9) is based on the reduced buckling length  $l_{cr} = L_1$  (see Fig. 5).

$$M_{II} = N_{1,Rd} \cdot f_M \cdot e_0 \cdot f_{II} = N_{1,Rd} \cdot \frac{1}{1 + \frac{I_{z,KB2}}{I_{z,KB1}}} \cdot \left( \frac{t_{KB1} + t_{KB2}}{2} \right) \cdot \frac{1}{1 - \frac{N_{1,Rd}}{N_{cr,BC2}}} \quad (8a)$$

$$M_{II} = N_{1,Rd} \cdot \frac{1}{1 + \frac{b_{eff} \cdot t_{KB2}^3}{h_{KB} \cdot t_{KB1}^3}} \cdot \left( \frac{t_{KB1} + t_{KB2}}{2} \right) \cdot \frac{1}{1 - \frac{N_{1,Rd}}{N_{cr,BC2}}} \quad (8b)$$



$$M_{II} = N_{t,Rd} \cdot e_t = N_{t,Rd} \cdot \frac{t_{KB1}}{5,14} \cdot \left( \frac{t_{KB1}}{20} \right)^3 \quad (10)$$

Table 2: Compression load capacity ratios  $N_{Rd} / N_{pl,0}$  (RHS - profile 100/100/5,  $b_{eff} = 330\text{mm}$ ), with imperfections as well as based on an engineering model for 3 variants:

-  $t_{KB1} = t_{KB2} = 12\text{ mm}$  (V1), -  $t_{KB1} = t_{KB2} = 20\text{ mm}$  (V2), -  $t_{KB1} = 20 / t_{KB2} = 12\text{ mm}$  (V3).

boundary cond.	calculation	slenderness $\bar{\lambda}_{z0}$											
		0,548			1,097			1,645			2,194		
		V1	V2	V3	V1	V2	V3	V1	V2	V3	V1	V2	V3
BC 1	GMNIA	0,161	0,309	0,367	0,163	0,302	0,357	0,160	0,272	0,295	0,148	0,177	0,183
	Eng. model	0,172 +6,8%	0,309 +0,0%	0,373 +1,6%	0,172 +5,5%	0,309 +2,3%	0,373 +4,5%	0,172 +7,5%	0,276 +1,5%	0,291 -1,4%	0,172 +16%	0,172 -2,8%	0,178 -2,7%
BC 2	GMNIA	0,526	0,825	0,643	0,525	0,654	0,643	0,361	0,425	0,424	0,219	0,286	0,275
	Eng. model	0,458 -13%	0,786 -4,7%	0,545 -15%	0,458 13%	0,598 -8,6%	0,545 15%	0,318 12%	0,318 -25%	0,318 -25%	0,188 -14%	0,188 -34%	0,188 -31%

## 6 CONCLUSION

The almost centric joint in Fig. 1 only for RHS - members in tension gives a load bearing capacity comparable with the section capacity  $N_{pl,0}$  (about 90 % of  $N_{pl,0}$ ). However, thick gusset plates are necessary, leading to an area ratio of  $A_{KB1} / A_0 > 1,25$ .

Also for such thick gusset plates with pinned ends the load bearing capacity in compression is limited to about 50 % of the section capacity  $N_{pl,0}$ , independent of the member slenderness. The reason for that is the high additional bending moment in the gusset plate at the member end (axis II in Fig. 5).

In case of a fixed gusset plate a maximum of about 70÷80 % of the section capacity  $N_{pl,0}$  is available. Only for very high member slenderness ( $\bar{\lambda}_{z,0} > 1,5 / 1,0$  for pinned / fixed gusset plates) the buckling check of the member is relevant for design.

It should be noted that the studied joint configuration of Fig. 1 is nearly not usable, if fatigue loads are relevant (stress cycles due to axial force). The reason for this, are very high stress peaks near the welds, relevant for the fatigue check.

## REFERENCES

- [1] Unterweger, H. and Ofner, R., "Traglast von Verbandsstäben aus Hohlprofilen mit quasi-zentrischem Knotenblechanschluss", *Stahlbau*, 78(6), 425-436, 2009.
- [2] ABAQUS, Software package, Version 6.7, 2007.
- [3] Eurocode 3, European Standard, *Design of steel structures – Part 1-1: General rules and rules for buildings*, 2006.
- [4] Wilkinson, T., "The plastic behaviour of cold – formed rectangular hollow sections", Doctoral Thesis, University of Sydney, 1999.